Sensorless Control of a Novel Linear Magnetostrictive Motor

Ali Sadighi, *Member, IEEE*, and Won-jong Kim, *Senior Member, IEEE*

***Abstract*—In this paper, the sensorless control of a novel linear magnetostrictive motor is presented. We developed this low-power linear magnetostrictive motor with local three-phase excitation. In response to a traveling magnetic field inside the Terfenol-D active element, it moves in the opposite direction with a peristaltic motion. It is observed that there is a direct relationship between the active element's position and the coils' inductances. To detect the inductance change, the coil's current response to a pulse voltage input is monitored. Then, a fundamental relationship between the coils' current-response pulsewidths and the active element's position is experimentally developed. Eventually, the closed-loop sensorless control of the linear magnetostrictive motor was successfully performed. The sensorless control demonstrated the position-estimation capability with a ±1-mm maximum error.**

***Index Terms*—Linear motors, magnetostriction, relay control systems, sensorless control.**

I. Introduction

OPERATING electric motors in harsh environments at high temperature and pressure poses a serious challenge in the reliable use of conventional sensors [1]. To overcome this problem, sensorless techniques have been developed where the mechanical position or speed sensors are eliminated by an electronic method [2]. The main idea behind most sensorless techniques is to find a fundamental relationship between the motor's position and its magnetic characteristics. By monitoring variables such as the current from either energized or unenergized phases, it is possible to track the changes in the magnetic characteristics of the motor [3]. In the energized-phase methods, the variables from the phases which generate torque or force are employed for position estimation [4]. In most unenergized-phase techniques, the phase inductance in an unenergized phase is measured and used for position estimation [5]. In these techniques, generally, a probing signal has to be injected to the unenergized phases for inductance calculation. Then, the relationship between the motor's position and the phase inductance is used to estimate the position.

Manuscript received October 1, 2009; revised December 17, 2009 and June 9, 2010; accepted August 27, 2010. Date of publication December 30, 2010; date of current version March 18, 2011. Paper 2009-EMC-311.R2, presented at the 2009 IEEE Energy Conversion Congress and Exposition, San Jose, CA, September 20–24 and approved for publication in the IEEE Transactions on Industry Applications by the Electric Machines Committee of the IEEE Industry Applications Society.

A. Sadighi is with the Department of Mechanical Engineering, University of Minnesota, Minneapolis, MN 55455 USA (e-mail: asadighi@umn.edu).

W. Kim is with the Department of Mechanical Engineering, Texas A&M University, College Station, TX 77843-3123 USA (e-mail: wjkim@tamu.edu).

Color versions of one or more of the figures in this paper are available online at http://ieeexplore.ieee.org.

Digital Object Identifier 10.1109/TIA.2010.2102732

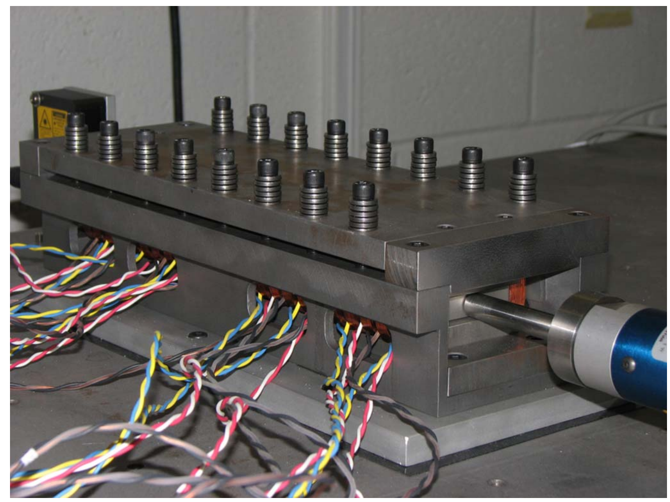

Fig. 1. Photograph of the linear magnetostrictive motor.

We developed a novel linear magnetostrictive motor using a rectangular slab of Terfenol-D as the active element [6] as shown in Fig. 1. Terfenol-D is an alloy of formula $Tb_{0.3}Dy_{0.7}Fe_{1.92}$ which was developed by the Naval Ordnance Laboratory and has the highest magnetostriction of any alloy, up to 2000 ppm [7], [8]. The linear magnetostrictive motor has demonstrated a speed of 9 mm/min with a load capacity of 410 N and a 45-mm travel range. The maximum power consumption by this motor is 95 W [6].

The aim of this paper is to develop a sensorless method for the closed-loop position control of the linear magnetostrictive motor. Based on an observation that illustrates a direct relationship between the motor's position and the coils' inductances, a fundamental relationship is developed between the motor's position and the coils' current-response pulsewidths. Then, an algorithm is proposed to estimate the motor's position based on the current-response pulsewidths.

In the following section, we present the working principle and electromagnetic design of the linear magnetostrictive motor. Section III describes the sensorless position estimation. The sensorless closed-loop position control of the linear magnetostrictive motor is presented and discussed in Section IV. Eventually, an application of the linear magnetostrictive motor with sensorless control is illustrated in Section V.

II. Linear Magnetostrictive Motor

An exploded view of the linear magnetostrictive motor and its working principle are shown in Fig. 2. This peristaltic motion of the active element could be induced by generating a traveling magnetic field. The active element in our design is a

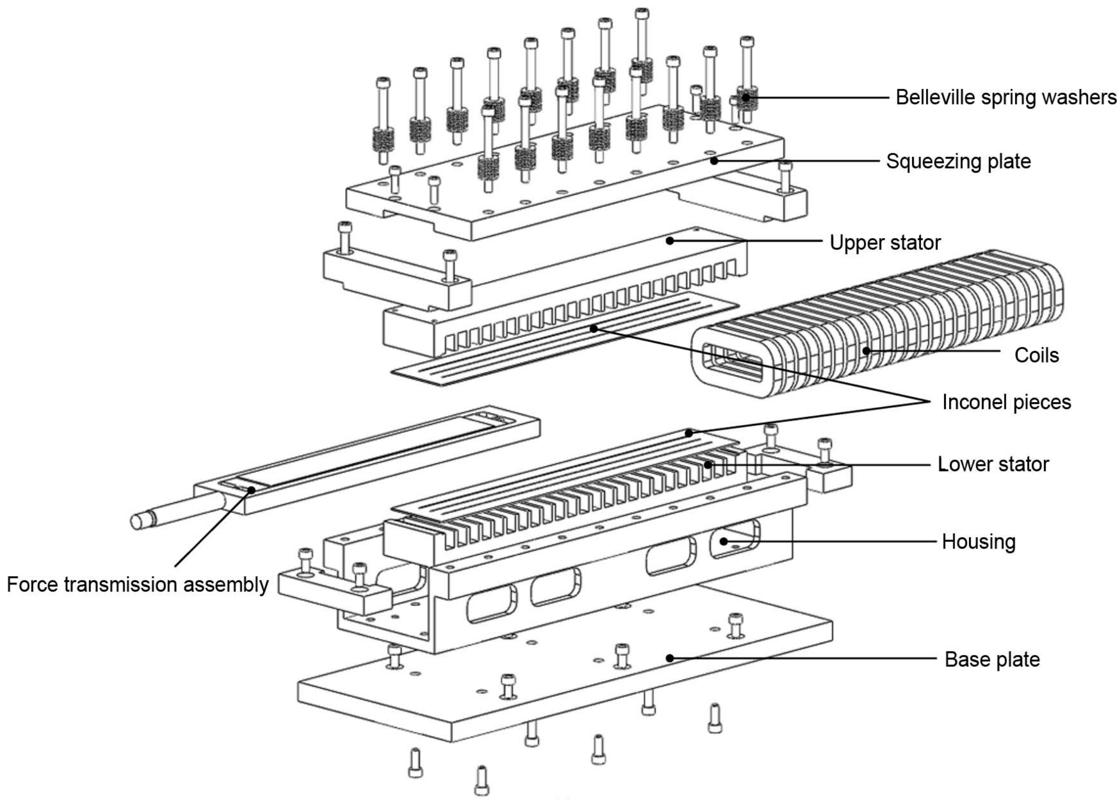

(a)

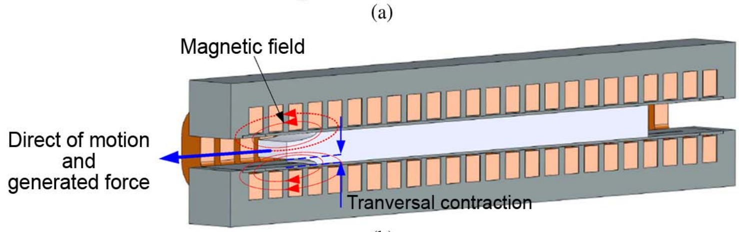

(b)

Fig. 2. (a) Exploded view of the linear magnetostrictive motor. (b) Working principle of the linear magnetostrictive motor.

rectangular slab surrounded by a force-transmission assembly. The active element is sandwiched between two thin sheets of Inconel-718 which are resistant to corrosion. The squeezing force is generated using 16 sets of Belleville spring washers and screws and transmitted to the active element through a squeezing plate. This squeezing force is transformed to the friction force between the active element and the Inconel pieces, which contributes to the reaction force required to move the active element against a load or to hold it in place. As a result, this motor self-brakes when the power is cut off, which is one of the major advantageous features of this linear magnetostrictive motor. The stators are made of solid Nickel–Iron Alloy 49 that has a very high relative permeability of 100 000 as well as good mechanical properties (tensile yield strength of 154 MPa) which makes it withstand normal and shear stresses due to the squeezing pressure and the external load.

The magnetic field is generated inside the active element by means of 24 prefabricated coils. To make the magnetic field travel, three power-electronics switching boards were constructed. The switching frequencies of these boards are controlled by the digital I/Os of a digital-signal-processing (DSP) board (Model DS1104 by dSPACE). Depending on the desired motion direction, the power electronics directs the current to three adjacent coils, and then, a traveling magnetic field is generated. Since only three out of the 24 coils are energized at each time, the power consumption of this linear motor is very low. The maximum power consumption by the linear magnetostrictive motor is 95 W [6]. The linear magnetostrictive motor has demonstrated a force-generating capability of 410 N, and the maximum speed is 9 mm/min.

A finite-element-analysis (FEA) tool was employed to simulate the linear magnetostrictive motor. The magnetostrictive geometry was modeled in a GiD preprocessor, and then, ATILA was used to solve the magnetomechanical coupling in the active element [9]. The simulation results for the local three-phase excitation of the linear magnetostrictive motor are shown in Fig. 3. As the magnetic field comes to interact with the active element, it results in the transversal contraction of that portion and, consequently, the longitudinal extension of the active element. Then, the magnetic field is moved to the other end, resulting in the overall displacement of the active element. In the first FEA result from the top in Fig. 3, none of the coils are excited. In the second FEA result from the top, coils #2, #3, and #4 are excited with a peak current equal to 2.5 A. In the third to the fifth FEA results, coils #3, #4, #5; #4, #5, #6; and #5, #6, #7 are excited with the same coil current, respectively.

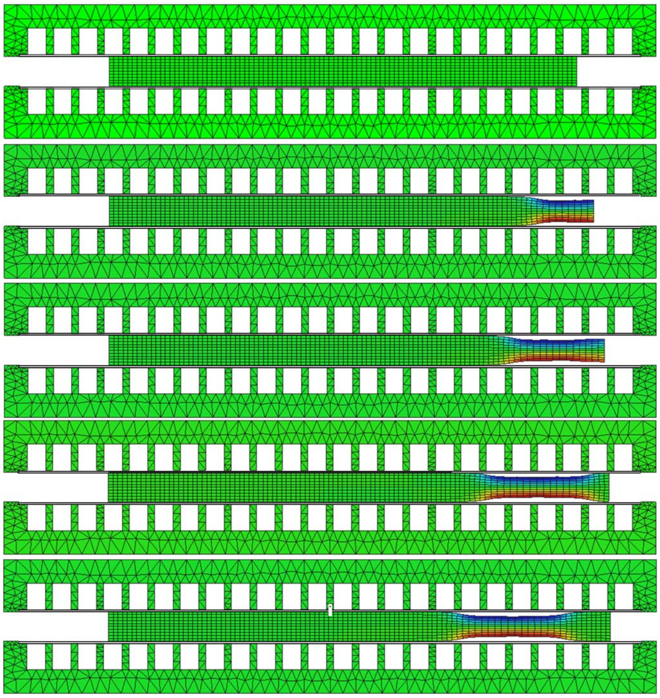

Fig. 3. FEA of the local three-phase excitation of the linear magnetostrictive motor (the magnetostriction is exaggerated by a factor of a million for the sake of clarity). Three adjacent coils are excited from the right with $i = 2.5$ A in each coil.

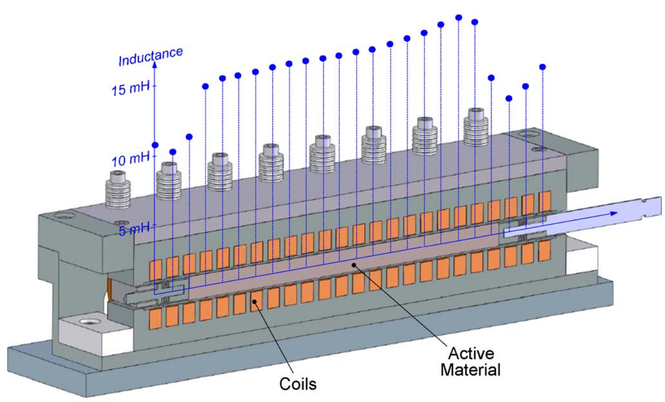

Fig. 4. Coils' inductance-measurement results with the active element placed in a predefined position illustrate the fundamental relationship between the motor position and its magnetic characteristics.

III. Sensorless Position Estimation

Most sensorless techniques are based on the development of a fundamental relationship between the motor position or speed and its magnetic characteristics. In search for such a relationship in the linear magnetostrictive motor, the active element was placed at a predefined position, and the coils' inductances were measured using an RCL meter. The cross section of the linear magnetostrictive motor with the active element at such a predefined position and the coils' inductance measurements are shown in Fig. 4.

The inductances of the coils which the active element is completely through were measured to be about 16 mH. In comparison, the inductances of the other coils are around 10 mH. It is apparent that the increase in the coils' inductances is due

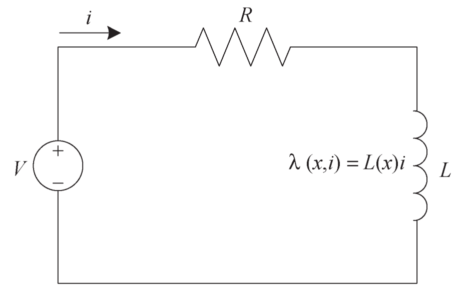

Fig. 5. Equivalent circuit of one coil.

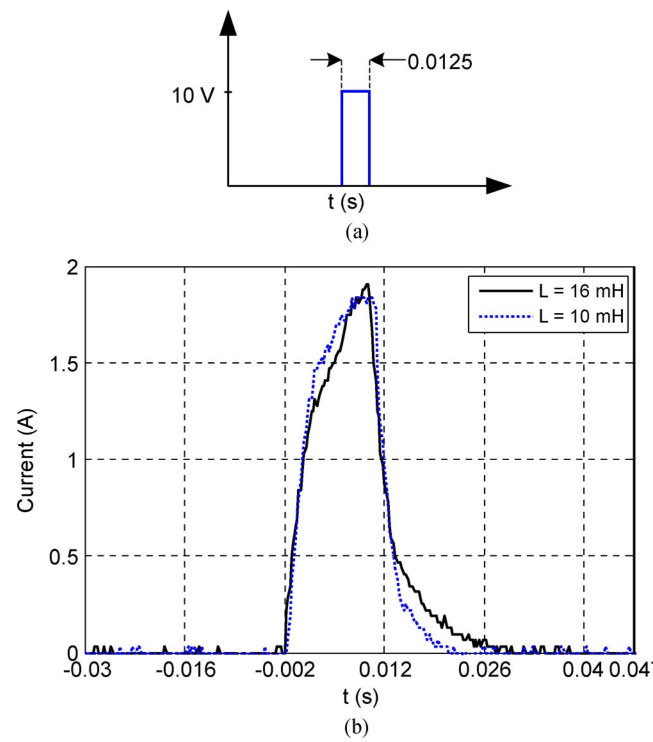

Fig. 6. (a) Pulse voltage input. (b) Current responses of two coils with different inductances to the same pulse voltage input.

to the relative permeability of Terfenol-D of three to ten. This implies that the linear magnetostrictive motor position can be inferred if we can detect the change in the coil inductances.

The equivalent circuit for a single coil is shown in Fig. 5. The terminal voltage for a single coil is written as

$$V = Ri + \frac{d\lambda}{dt} \tag{1}$$

where R is the coil resistance and λ is the flux linkage linked by the coil. Since the flux linkage is a function of the coil current and the active element's position, we may rewrite the equation as

$$V = Ri + \frac{\partial\lambda}{\partial i}\frac{di}{dt} + \frac{\partial\lambda}{\partial x}\frac{dx}{dt} \tag{2}$$

where the second and third terms are the transformer voltage and the speed voltage, respectively [10]. Equation (2) is rearranged as an expression for the rate of change of the coil current

$$\frac{di}{dt} = \frac{V - Ri - \frac{\partial\lambda}{\partial x}\frac{dx}{dt}}{\frac{\partial\lambda}{\partial i}}. \tag{3}$$

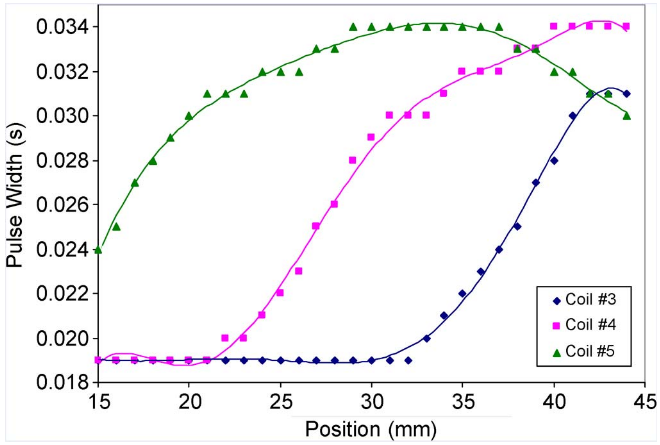

Fig. 7. Recorded current-response pulsewidths for three coils when the active element's position changes from 15 to 45 mm.

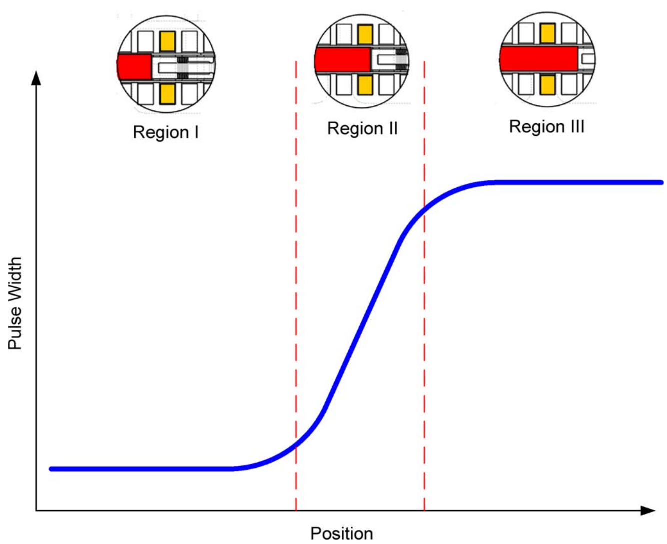

Fig. 8. Three regions of a current-response pulsewidth versus position curve.

Considering the low speed of the linear magnetostrictive motor (9 mm/min), the speed voltage term can be neglected. In addition, by assuming the system to be electrically linear, the flux linkage can be described as

$$\lambda = L(x)i \tag{4}$$

and, thus,

$$\frac{di}{dt} \approx \frac{V - Ri}{L(x)}. \tag{5}$$

Since the generalized inductance $L(x)$ of a coil is a function of position, the rate of change of the coil current is also a function of position.

The responses of two motor coils with different inductance values to a pulse voltage input are shown in Fig. 6. As it is seen, by increasing the coil's inductance from 10 to 16 mH, the current-response pulsewidth rises from 0.020 to 0.030 s. Thus, the current-response pulsewidth can be considered as a representation of the magnetic characteristics of the linear magnetostrictive motor. Hence, the fundamental relationship will consist of a relationship between the coils' current-response pulsewidth and the motor position.

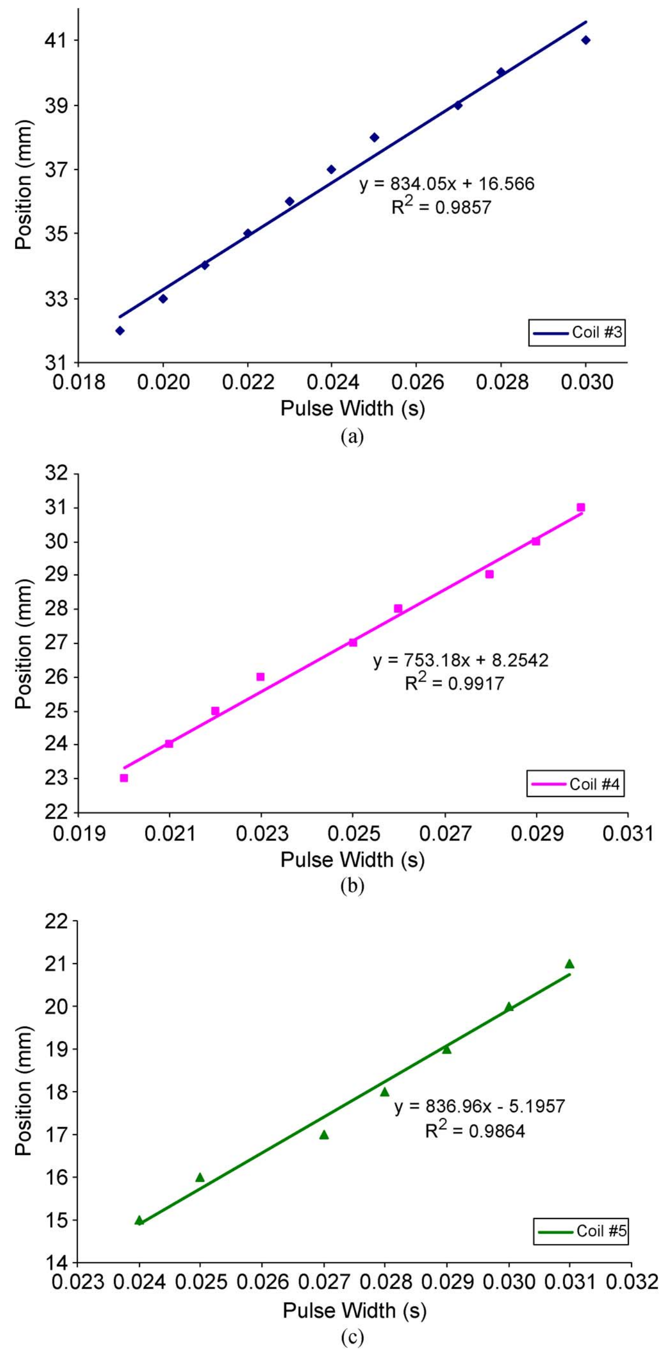

Fig. 9. Linear regions of the coils and their corresponding equations. (a) Coil #3. (b) Coil #4. (c) Coil #5.

To find this fundamental relationship, we changed the active element's position from 15 to 40 mm, and the current-response pulsewidths of coils #3, #4, and #5, denoted by t_3, t_4, and t_5, were recorded with 1-mm increments. To measure the coil current, we used Hall-effect-based transducers (model LA 03-PB from LEM). The results are depicted in Fig. 7. To avoid noise interference, the current-response pulsewidth was measured from the time that the current goes beyond 0.1 A until it falls below the same value and the drive voltage was 10 V.

For each pulsewidth curve as shown in Fig. 7, there are three regions. The first is the low-magnitude region with a pulsewidth of around 0.020 s (Region I). This region corresponds to the active element not inside the coil yet. Then, there is an increasing

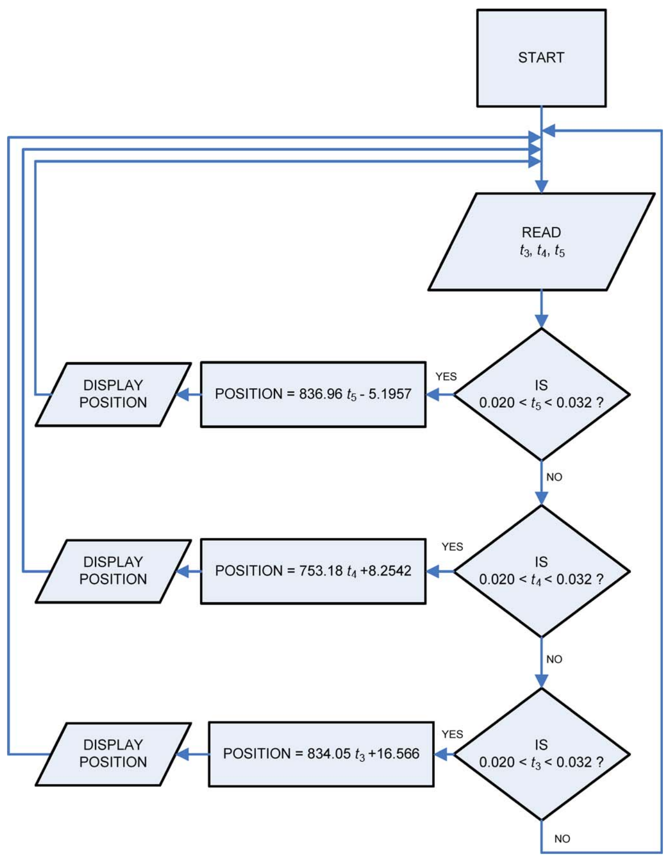

Fig. 10. Position estimation flowchart.

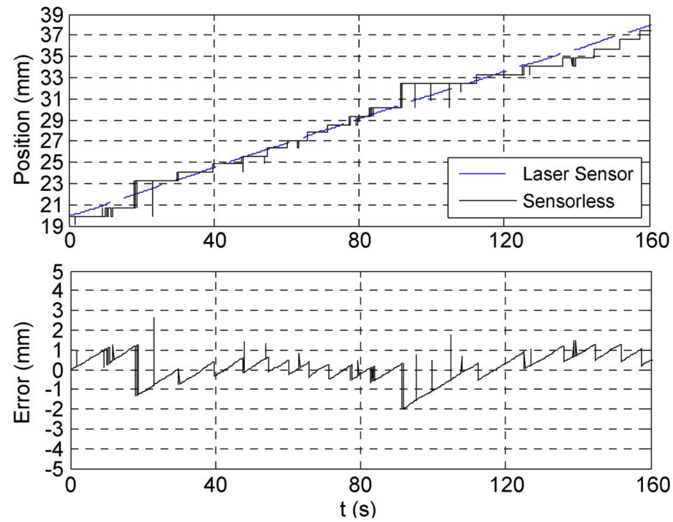

Fig. 11. Sensorless position estimation error.

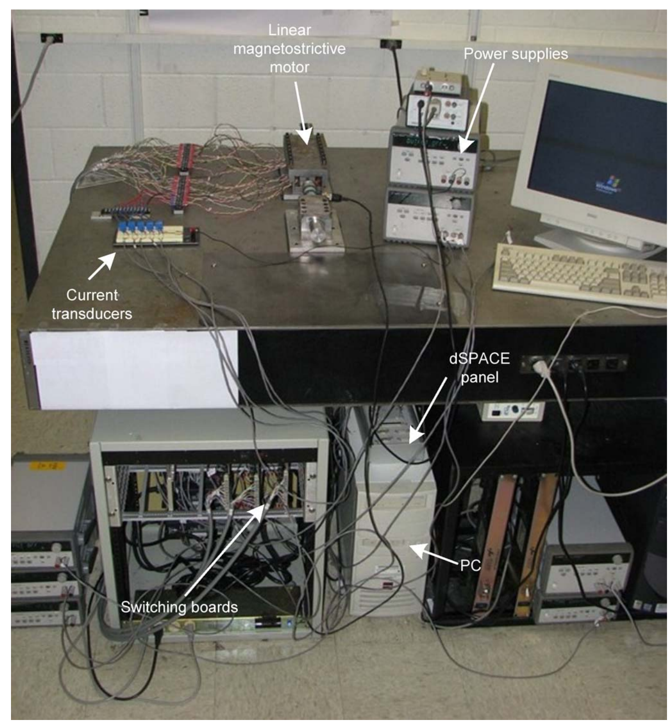

Fig. 12. Photograph of the test setup.

region which starts from the time that the active element begins entering the coil until it is completely through the coil (Region II). Finally, each curve saturates at a pulsewidth of around 0.032 s, which corresponds to the active element being completely through the coil (Region III). These three regions for one coil are depicted in Fig. 8.

To derive the fundamental relationship between the active element's position and the current-response pulsewidths, a line was curve fitted to the linear region (Region II) of each curve as shown in Fig. 9. The active element's position in the three linear regions of coils #3, #4, and #5 can be estimated by

$$\text{position} = 834.05 t_3 + 16.566 \tag{6}$$
$$\text{position} = 753.18 t_4 + 8.2542 \tag{7}$$
$$\text{position} = 836.96 t_5 - 5.1957 \tag{8}$$

with R^2 values of 0.9857, 0.9917, and 0.9864, respectively. These values indicate that relying on this linear estimation is quite effective in establishing the fundamental relationship between the position and the current-response pulsewidth.

The position calculation flowchart is shown in Fig. 10. The output voltages of the current transducers are sent to the analog-to-digital (A/D) converters. The pulsewidths of coils' current responses are measured and denoted by t_3, t_4, and t_5 in the flowchart. As shown in the flowchart, the algorithm detects the coil in Region II and then uses the corresponding linear equation to calculate the position.

To verify the effectiveness of the proposed algorithm to infer the position, the motor position was changed, and the measurement from a laser distance sensor was compared with the estimated position. The sensorless position measurement versus the laser distance sensor output and the error are depicted in Fig. 11. As it is seen, by employing this methodology, we are able to infer the position of the linear magnetostrictive motor with a ±1-mm maximum error. This error is partially due to the linear approximation that we made earlier in developing the relationship between the current-response pulsewidth and the position. The other factor that contributes to the error in the sensorless position calculation is that a minimum change in the active element's position should be made before a change in the current-response pulsewidth could be detected. The spikes in the inferred position are due to the errors in current sensing but do not much affect the closed-loop performance of the linear magnetostrictive motor as we will see in the following section.

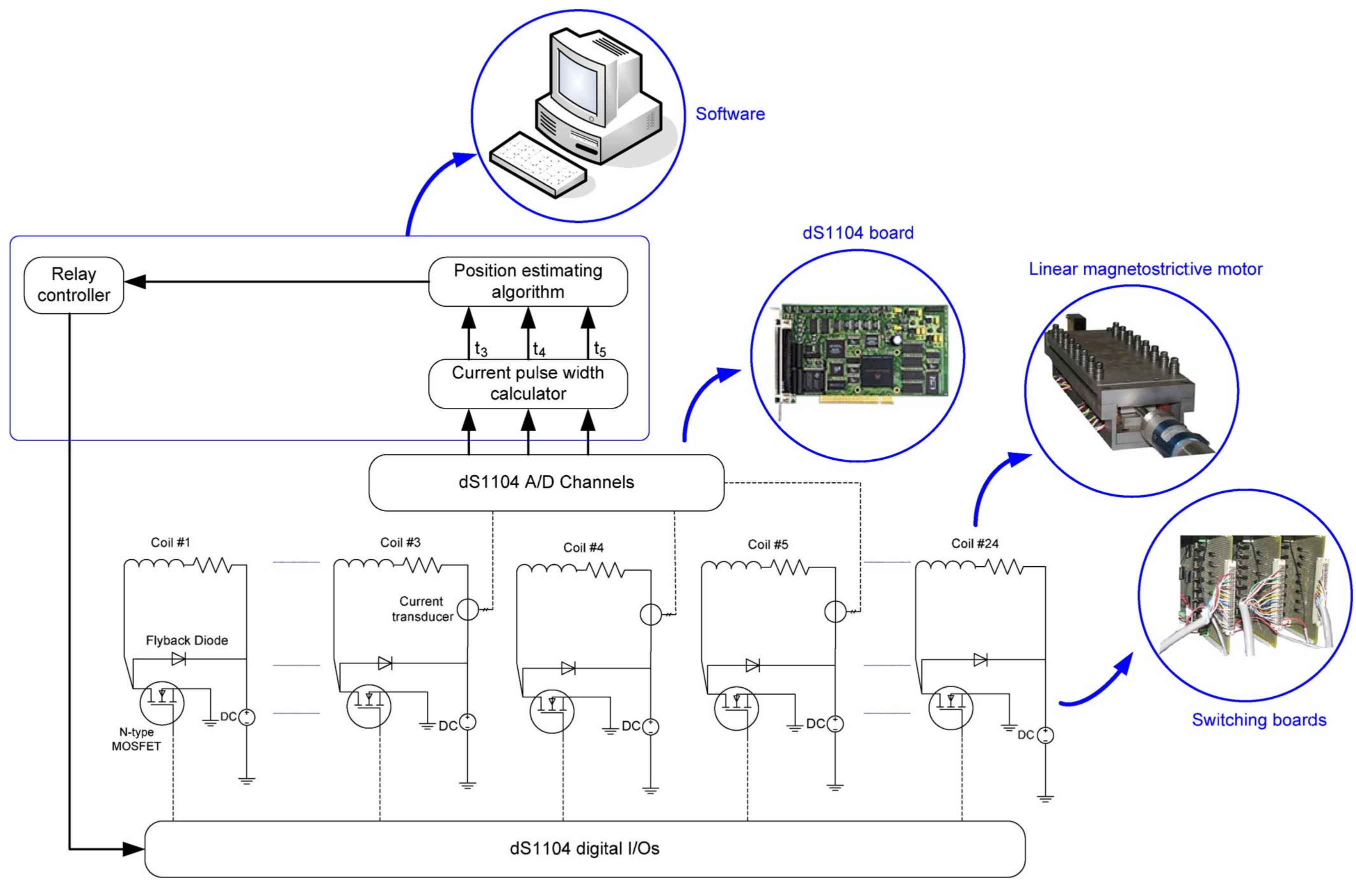

Fig. 13. Schematic control and instrumentation diagram.

IV. Sensorless Closed-Loop Control

Now, the position-estimation algorithm could be used to implement the closed-loop control of the linear magnetostrictive motor. A photograph of the test setup is shown in Fig. 12. The schematic diagram of the control and instrumentation is shown in Fig. 13. Each coil of the motor consists of 273 turns of AWG#24 wire, and each switching board contains eight power metal–oxide–semiconductor field-effect transistors (MOSFETs) (model IRF3315Pbf by International Rectifier) and eight MOSFET drivers (model TC4420 by Microchip).

The coil currents are measured using Hall-effect-based current transducers, and the output voltages are sent to the A/D converters of the DSP board. Then, the current pulsewidths t_3, t_4, and t_5 are calculated and sent to the position estimation algorithm. The estimated position is then fed back to a relay controller with a dead zone defined as

$$u = \Phi(e) = \begin{cases} +1, & e > k_0 \\ 0, & -k_0 < e < k_0 \\ -1, & e < -k_0 \end{cases} \tag{9}$$

where $\pm k_0$ defines the dead zone of the relay element. Since the precision of the position monitoring system is ± 1 mm, a dead-zone threshold value of 1 mm should be picked to avoid self oscillation [11].

Fig. 14 depicts a 5-mm closed-loop step response of the linear magnetostrictive motor with the sensorless position estimator. The steady-state error is only 0.65 mm which is within the ± 1-mm maximum error boundary as expected. This relay-based controller is also robust to the spikes present in the estimated position as seen in Fig. 11. That lies in the fact that the spikes are of random nature and do not always appear at the same position where the motor operates. Hence, although, in some instances, the error signal changes due to spikes, they do not much affect the relay control signal output. This control

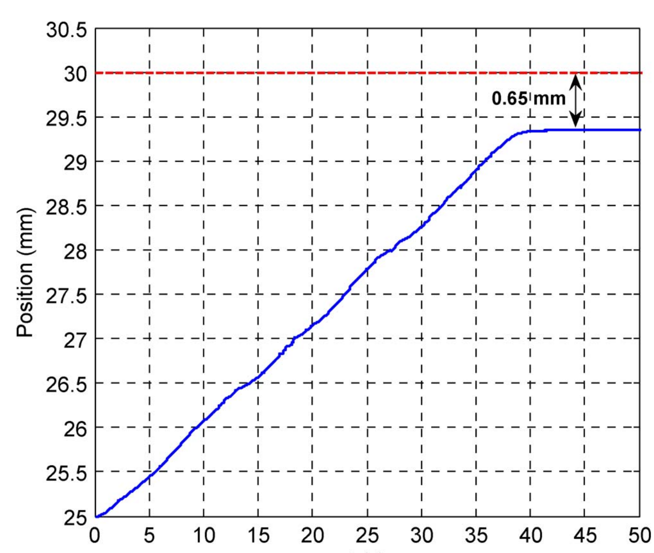

Fig. 14. Five-millimeter step response of the linear magnetostrictive motor with sensorless control.

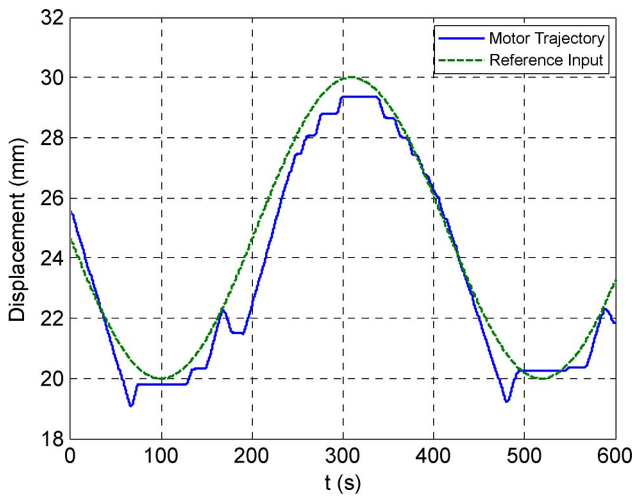

Fig. 15. Closed-loop response to a sinusoidal reference input with an amplitude of 5 mm and a frequency of 15 mrad/s.

output is always at maximum and makes the motor move in the desired direction at the maximum speed until it reaches the vicinity of the reference input as specified by the dead-zone threshold.

Fig. 15 shows the capability of the sensorless control system in tracking a sinusoidal reference input with an amplitude of 5 mm and a frequency of 15 mrad/s. The proposed sensorless control results in the successful tracking of a sinusoidal reference input. Nevertheless, in some instances, the error goes beyond the expected value of ± 1 mm which is due to the low speed of the motor. As it is seen in the figure, in peak points, the error is within ± 1 mm.

V. Application

One of the potential applications of the linear magnetostrictive motor is to actuate the sliding-sleeve valve (SSV) [12] used to establish or cut off the communication between the tubing and the annulus in an oil well [1]. A schematic drawing of the SSV is shown in Fig. 16.

By means of the linear magnetostrictive motor, the sleeve could be shifted to open or close the ports machined in the body of the valve. Using the linear magnetostrictive motor with sensorless control has two main benefits for this application. First, the power consumption of the motor is quite low, and it self-brakes when the power is cut off [6], which suit the power supply limitations in down-hole applications. Second, the sensorless position monitoring and control eliminates the need for using conventional sensors in a harsh down-hole environment, which adds to the complexity and decreases the reliability of the actuation system.

In the schematic SSV shown in Fig. 16, the sleeve can be shifted to five different levels (L_1 to L_5) to control the fluid flow from zero to maximum. Fig. 17 shows the trajectory of the linear magnetostrictive motor with sensorless control to change the valve status from fully open to fully close. In all five levels, the steady-state error is less than 1 mm. Since the distance between two adjacent ports, γ, is larger than 2 mm, the sleeve could be situated in the area between two ports using the sensorless position estimation.

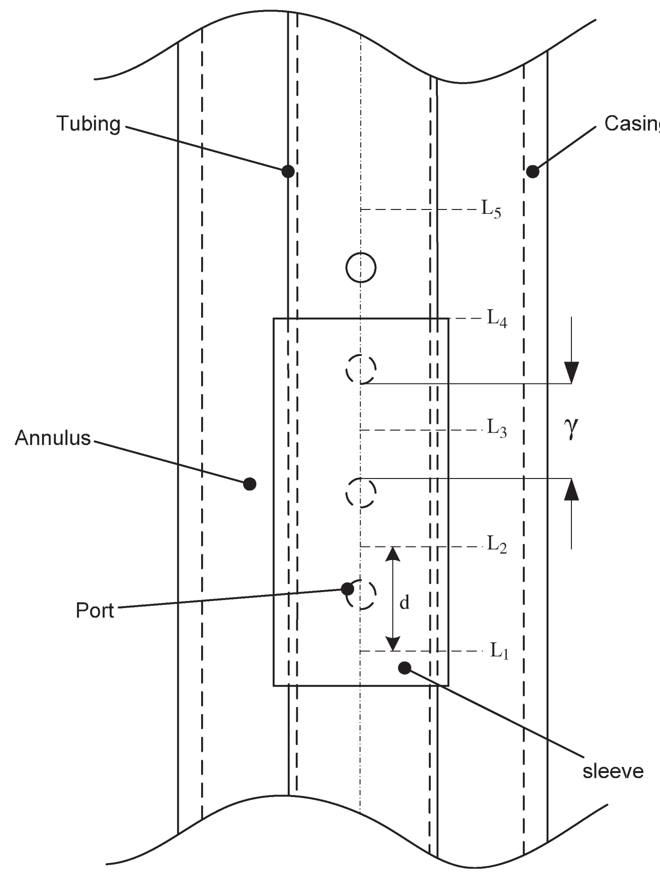

Fig. 16. Schematic drawing of an SSV.

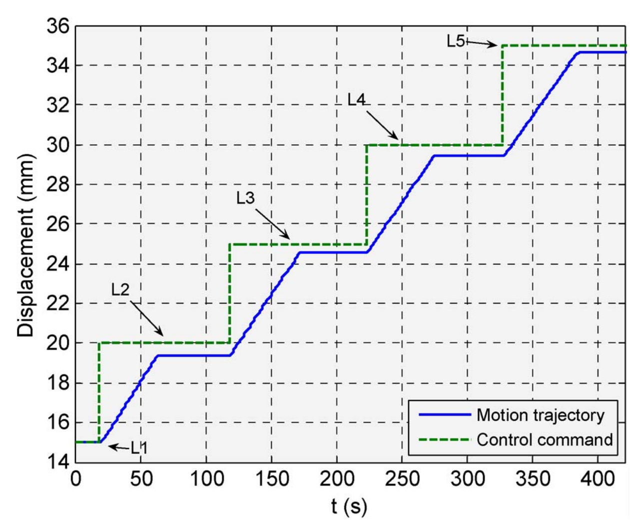

Fig. 17. Control command to situate the SSV at L_1, L_2, L_3, L_4, and L_5 and the motor's actual motion trajectory.

VI. Conclusion

A novel sensorless control methodology was successfully developed and implemented for a linear magnetostrictive motor. First, the relationship between the inductance change in motor coils and the active element's position was measured. Based on this measurement with multiple sets of experiments, a fundamental relationship between the coils' current-response pulsewidths and the active element's position was established.

Using the linear regions of the fundamental relationship, an algorithm was proposed to infer the linear magnetostrictive motor's position. The proposed method demonstrated a maximum position-estimation error band of ± 1 mm. The closed-loop control of the linear magnetostrictive motor was successfully performed by feeding the inferred position back to a relay controller. Finally, a down-hole application was discussed with an SSV to be actuated using the sensorless control of the linear magnetostrictive motor.

ACKNOWLEDGMENT

The authors would like to thank Prof. H. A. Toliyat of Texas A&M University for allowing them to use the RCL meter in the Electrical Machines and Power Electronics Laboratory.

REFERENCES

[1] D. Perrin, *Well Completion and Servicing*. Paris, France: Editions Technip, 1999.

[2] K. Rajashekara, A. Kawamura, and K. Matsuse, *Sensorless Control of AC Motor Drives*. New York: IEEE Press, 1996.

[3] T. J. E. Miller, *Electronic Control of Switched Reluctance Machines*. Woburn, MA: Reed, 2001.

[4] N. Ertugrul and P. Acarnley, "A new algorithm for sensorless operation of permanent magnet motors," *IEEE Trans. Ind. Appl.*, vol. 30, no. 1, pp. 126–133, Jan. 1994.

[5] P. P. Acarnley, R. J. Hill, and C. W. Hooper, "Detection of rotor position in stepping and switched motors by monitoring of current waveforms," *IEEE Trans. Ind. Electron.*, vol. IE-32, no. 3, pp. 215–222, Aug. 1985.

[6] W.-J. Kim and A. Sadighi, "A novel low-power linear magnetostrictive actuator with local three-phase excitation," *IEEE/ASME Trans. Mechatronics*, vol. 15, no. 2, pp. 299–307, Apr. 2010.

[7] F. Claeyssen, N. Lhermet, and G. Grosso, "Giant magnetostrictive alloy actuators," *J. Appl. Electromagn. Mater.*, vol. 5, pp. 67–73, 1994.

[8] F. Claeyssen, N. Lhermet, R. Le Letty, and P. Bouchilloux, "Actuators, transducers and motors based on giant magnetostrictive materials," *J. Alloys Compd.*, vol. 258, no. 1/2, pp. 61–73, Aug. 1997.

[9] K. Uchino, *FEM and Micromechatronics With ATILA Software*. Boca Raton, FL: CRC Press, 2008.

[10] H. H. Woodson and J. R. Melcher, *Electromechanical Dynamics*. New York: Wiley, 1968.

[11] W.-J. Kim and A. Sadighi, "Design and relay-based control of a novel linear magnetostrictive motor," in *Proc. Amer. Control Conf.*, Jun. 2009, pp. 3482–3487.

[12] A. P. Dorel, "Linear actuator using magnetostrictive power element," U.S. Patent 7 675 253 B2, Mar. 9, 2010.

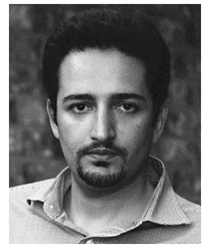

Ali Sadighi (S'08–M'10) was born in Yazd, Iran, in 1978. He received the B.S. degree in mechanical engineering from Sharif University of Technology, Tehran, Iran, in 2000, the M.S. degree in mechanical engineering from K. N. Toosi University of Technology, Tehran, in 2003, and the Ph.D. degree in mechanical engineering from Texas A&M University, College Station, in 2010. He also received the Certificate in Business from Mays Business School, Texas A&M University.

From 2003 to 2006, he was a Design Engineer with MAPNA, Tehran. He is currently a Postdoctoral Associate in the Department of Mechanical Engineering, University of Minessota, Minneapolis. His current research interests include the design, modeling, and control of mechatronic systems.

Dr. Sadighi is a member of the American Society of Mechanical Engineers (ASME) and Phi Kappa Phi. He was also the recipient of the Best Student Paper Finalist Award at the 2010 IEEE/ASME International Conference on Advanced Intelligent Mechatronics.

Won-jong Kim (S'89–M'97–SM'03) received the B.S. (*summa cum laude*) and M.S. degrees in control and instrumentation engineering from Seoul National University, Seoul, Korea, in 1989 and 1991, respectively, and the Ph.D. degree in electrical engineering and computer science from the Massachusetts Institute of Technology (MIT), Cambridge, in 1997.

Since 2000, he has been with the Department of Mechanical Engineering, Texas A&M University (TAMU), College Station, where he is currently an Associate Professor and the Holder of the Dietz Career Development Professorship II. After receiving the Ph.D. degree, he was with SatCon Technology Corporation, Cambridge, for three years. His current research interests include the analysis, design, and real-time control of mechatronic systems, networked control systems, and nanoscale engineering and technology. He is the holder of three U.S. patents on precision positioning systems. He is an Associate Editor of the *ASME Journal of Dynamic Systems, Measurement, and Control*, and the *International Journal of Control, Automation, and Systems*.

Dr. Kim was the recipient of the Korean Institute of Electrical Engineers' Student Paper Contest grand prize in 1988, Samsung Electronics' Humantech Thesis gold prize for his MIT dissertation in 1997, the National Aeronautics and Space Administration Space Act Award in 2002, and the 2005 Professional Engineering Publishing Award for the best paper published in 2004 in the *Journal of Engineering Manufacture*. He was also a semifinalist in the National Institute of Standards and Technology's Advanced Technology Program competition in 2000. He was appointed as a Select Young Faculty Fellow by the TAMU College of Engineering and the Texas Engineering Experiment Station twice in 2003 and 2005. He was the recipient of the BP Teaching Excellence Award from TAMU College of Engineering in 2006. He is a member of Pi Tau Sigma and a Fellow of the ASME. He is a Technical Editor of the IEEE/ASME TRANSACTIONS ON MECHATRONICS.